Fusion Scheme for Pedestrian Safety in Urban Roads

Fernando Garcia, Daniel Olmeda, Aturo de la Escalera and José María Armingol
Intelligent System Lab
University Carlos III de Madrid
Leganes, Spain.
{fegarcia,dolmeda,armingol,escalera}@ing.uc3m.es

Abstract – Trustworthy sensors are the key points regarding road safety applications. The lack of reliable sensors able to fulfil the entire requirements for these situations makes fusion schemes mandatory. A fusion scheme that uses two sensors: far infrared camera vision and a laser scanner to perform pedestrian detection is presented. Both sensors have different field of view thus different detection zones are created according to the sensors available for detection in each zone. The proposed algorithm performs hybrid fusion by combining low and high level information. Experimental results show that combining both sensors detection is improved.

Keywords: Data association, hybrid systems, real-world applications.

1 Introduction

In recent years, advances in information technologies have lead to more complex applications, able to deal with a large variety of situations. ADAS (Advance Driver Assistant Systems) are the name of applications that help to both warm and prevent hazardous situations in road environments. In order to provide reliable ADAS one of the main tasks to be tackled is obstacle detection, especially those that represent the most vulnerable road users, pedestrians. Detecting those users and anticipate to potentially dangerous situations underlines the need to use different sensors combined to provide a reliable and accurate application able to fulfill requirements of such challenging applications. Here is where data fusion architectures are gaining importance, providing reliable and trustworthy data by combining different information sources.

The typical set of sensors used in road safety applications are laser scanners and computer vision. Laser scanners provide limited information but highly precise. Computer vision provides higher amount of data but less structured. Combining both sensors, these limitations can be overcome.

In this paper a fusion method is proposed. The method combines the information provided by a 2D laser range finder and far infrared (FIR) camera vision. This information is used to detect obstacles in road environments and differentiate when pedestrians are presented. The pedestrian detection is performed independently due to the difference in capabilities and distance ranges. In regions where ranges overlap, a fusion algorithm deals with the redundant information, increasing the positive detection results and avoiding false positives.

1.1 JDL Model for road applications

The number of works related with data fusion architectures for road safety applications has increased in the recent years. The new sensors available for driver environments and the new challenges related to road safety and driver technologies, as DARPA Grand Challenge and Urban Challenge have increased the research effort in these areas. However most of the works deal with the different applications avoiding sensor fusion theory. Only some approaches tries to develop a complete architecture that fulfill the requirements of typical data fusion applications. In [1] authors try to develop a specific scheme derived from de JDL model, specifically designed for road safety applications. The proposed model describes the different processes to be accomplished for fusion application in road environments. This model represents a tool for a fast and easy approximation to fusion architectures in road environments.

In the present work, standard JDL model is followed [2] and [3]. This paper is the first data fusion approach for the platform IVVI 2.0 developed by Intelligent System Lab from University Carlos III de Madrid. This platform has installed a laser scanner, a stereo camera system, a far infrared system and a color camera. These systems are used to test the algorithms developed by the Intelligent System Laboratory.

The presented work describes the implementation of levels 0, 1 and 2 of JDL data fusion model. It tries to develop a hybrid scheme that combines track to track high level detection adding some low level information to develop a feature vector which is introduced in an automatic learning Adaboost scheme.

2 State of the art

Fusion methods in road applications are typically divided in two sets according to the level in which fusion is performed. Low level Fusion schemes [4] perform fusion using a unique set of data extracted from both sensors. High level fusion schemes [5] perform fusion at track level.

Fusion schemes can also be differentiated in track based fusion and cell based fusion schemes. First tries to associate the different objects found in each sensor [6]. Second one [7] uses occupation grids, adding confidence according to the kind of sensor that detects the obstacle, but losing the geometrical structure.

Low level approaches that take advantage of statistical knowledge are presented in [4], [8] and [9], these approaches obtain information from all sensors and combine the information using whether Bayes formula, SVM, Neural Networks, etc …

Other works related to fusion schemes take advantage of laser scanner trustworthiness to select regions of interest where vision based systems try to detect pedestrians [10] and [11]. In [12] Detection of especially dangerous zones is done using laser scanner information integrated along time.

[13] Performs medium level fusion. It processes information from different sensors creating a feature vector which is used to perform an unique classification.

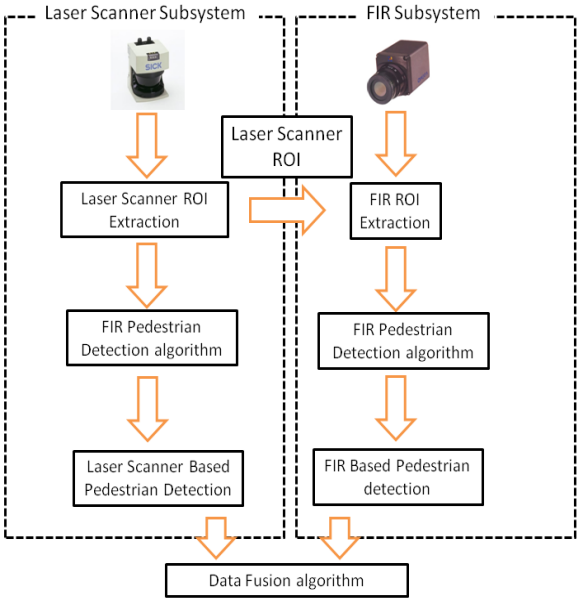

Figure 1. System Architecture.

3 General description

A hybrid fusion system is presented in this paper. Two detection subsystem detect pedestrian in a separate way and fusion is performed according to the zone where pedestrian are detected (figure 1).

--Laser Scanner subsystem, detects pedestrians using only data provided by Laser Scanner.

--FIR subsystem, detects pedestrians using information temperature provided by a FIR camera.

--Data Fusion algorithm processes the information from both subsystems and according to the position of the possible pedestrian, and low level information, performs data fusion.

3.1 Fusion Zone

Zone where both sensors are able to give detection information is called Fusion Zone (figure 2.A). Its range is from 5m to 30m.

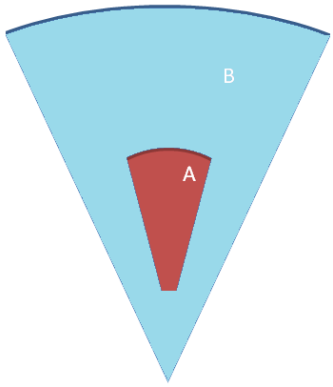

Figure 2. Detection Zones

Maximum distance is given by algorithm performance. Over 30 meters information is not enough to give a good detection. Below 5 meters, the camera is not able to give the complete shape of a typical pedestrian. Given an average height of a pedestrian of 1,70 meters, and a vision angle of the camera (19º) minimum distance is 5m.

$$\mathrm{tg}\left(\frac{\propto}{2}\right) = \frac{\frac{h}{2}}{d} \qquad d \approx 5\,meters \quad (1)$$

where h= 1.70 meters and α=19º.

Although eq. 1 supposes that FIR camera is located at the medium height of a human being. In real world it is not always in this way, but it is a good estimation of the distance in which the system has enough information to perform detection. Test performed to the FIR algorithm corroborates these assumptions and sets minimum detection distance at 5m.

3.2 Laser scanner zone

Field of view of laser scanner is considerably higher and wider. Model used was a LMS 291 S-05 from SICK. The laser scanner configuration was 100º of field of view, a maximum distance of 80 meters and an angular resolution of 0.25º. It gives a zone where only laser detection is performed (figure 2.B).

4 Subsystems descriptions

Information given by laser scanner is sufficient to provide a first estimation of the shape of the obstacle detected and even to provide some classification results. Besides the detection information, its trustworthiness can be used to provide interest regions that can be used both in laser scanner space and FIR image space.

The algorithm is composed by two stages. In the first stage, the data is received and a low level classification is performed. Data is integrated along time during the second stage, thus a high level classification is obtained giving more robust classification.

4.1.1 Stage 1.Low Level Detection

Four steps are followed during the first stage.

Egomotion Correction

Before environmental reconstruction using laser information, egomotion correction is mandatory to minimize distortions due to the time difference between the spots, data received by the laser is corrected according to the movement of the vehicle. Egomotion information is obtained from a GPS Sensor. It provides positioning data and egomotion information such as velocity, acceleration, Euler angles (absolute and angular velocity) etc... This information was used to compensate the movement of the car for each pulse separately (eq. 2 to 5):
Translation compensation:

$$x = x_0 - v \cdot T_i \cdot cos(\Delta\varphi) \quad (2)$$
$$y = y_0 - v \cdot T_i \cdot sen(\Delta\varphi) \quad (3)$$

Rotation compensation:

$$x = \cos(\Delta\varphi) \cdot x_0 - \sin(\Delta\varphi) \cdot y_0 \quad (4)$$
$$y = \sin(\Delta\varphi) \cdot x_0 + \cos(\Delta\varphi) \cdot y_0 \quad (5)$$

where v is the velocity of the car, T_i the time between a given spot and the first spot of a scan. And $\Delta\varphi$ is the increment in the pitch angle during a period of time T_i.

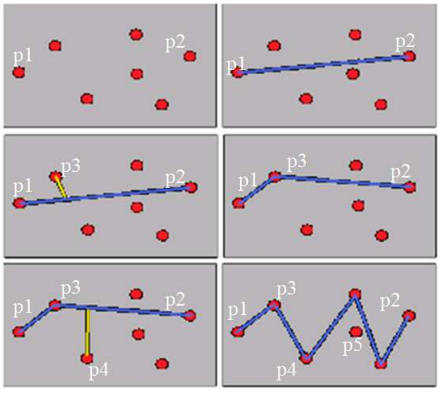

Figure 3. Polyline Creation process

Obstacle Detection

After egomotion correction, the resulting points are joined according to the distance among them. Clustering algorithm based on the Euclidean distance and a threshold which is distance dependant (eq. 6).

$$th = th_0 + K \cdot dist \quad (6)$$

here th_0 is the base threshold and K is a proportional constant which is multiplied by the distance.
Thus, for a given point $p(x_i,y_i)$ it may be treated as belonging to a segment S_j if it satisfies eq. 7:

$$p_i(x_i, y_i) \epsilon\, S_j \rightarrow \{\exists\, [\, p_j(x_j, y_j)\ \epsilon\, S_j\,] \colon d(p_j, p_i) < th\,\} \quad (7)$$

The algorithm checks for all every segment, if the case arises where a point is not included within any segment, a new segment is then created. Finally segments with only one point are eliminated while they are considered as false detection points.

Polyline creation

Once the segments are created, the points contained within each segment are merged using lines known as polylines. This process is a variation of the Ramer algorithm [14]. The first and last points are merged on a line, for each point contained within this segment, the distance to the line is checked and if it is higher than a given threshold two new lines are created merging these three points. This process is repeated for every point. Figure 3 shows an example. Distance from p3 to the line that connects p1 and p2, is higher than a threshold, so a new line is created. The same happens with every point but p5 which distance to the line is lower than this threshold.

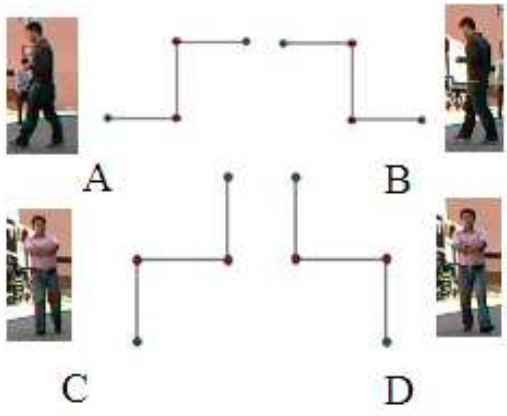

Figure 4. Models for lateral movement.

Low level classification

Low level classification is performed with the information provided by the polylines about the shape of the obstacles. Obstacles are differentiated in: Small obstacles, road borders, possible vehicles, L shaped obstacles, pedestrians and other obstacles. Detailed obstacle description can be found in [15] and [16].
For pedestrians detection two types are relevant, small obstacles and pedestrians. First could be considered as possible regions of interest (ROIs) that could contain a non detected pedestrian and that could be processed by another information source, i.e. FIR camera. Pedestrian

detections correspond to the obstacles that can be classified as pedestrians due to their shape. The algorithm used for this approach is based on the detection of two legs. The movement of a pedestrian is modeled using models of typical pedestrian walking.

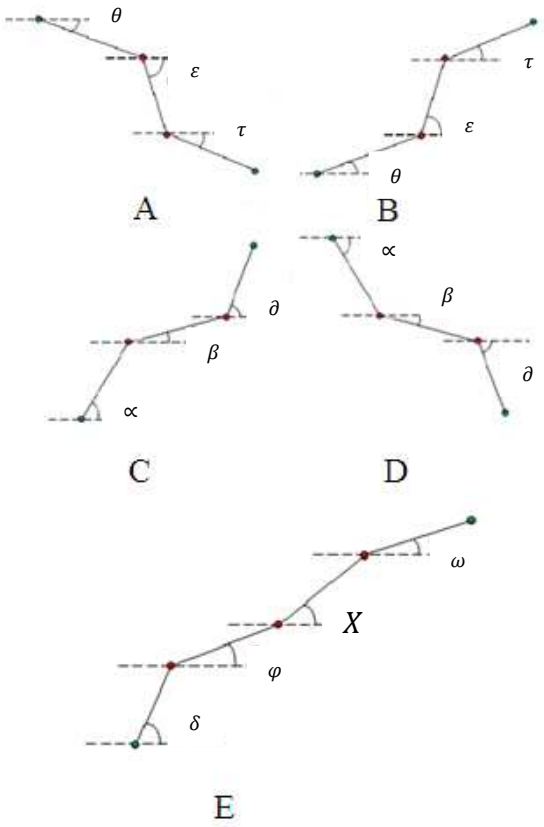

Figure 5. Models for the different movements.

Figure 4 shows the different possibilities taken into account. Figure 5 shows the models corresponding to each possibility shown in figure 4.The model used for four polylines is presented in figure 5 E. The angles allowed for those models are shown below:

For parallel movements:

$$45^o \leq \propto \leq 90^o$$
$$0^o \leq \beta \leq 55^o$$
$$45^o \leq \delta \leq 90^o$$

For perpendicular movements:

$$0^o \leq \theta \leq 55^o$$
$$35^o \leq \varepsilon \leq 90^o$$
$$0^o \leq \tau \leq 55^o$$

For four polylines segments two cases are taken into account:
Case 1:

$$35^o \leq \rho \leq 90^o$$
$$0^o \leq \varphi \leq 45^o$$
$$35^o \leq X \leq 90^o$$
$$0^o \leq \omega \leq 45^o$$

Case 2:

$$0^o \leq \rho \leq 45^o$$
$$35^o \leq \varphi \leq 90^o$$
$$0^o \leq X \leq 45^o$$
$$35^o \leq \omega \leq 90^o$$

4.1.2 Stage 2. Higher Level Classification

A higher level stage is required to observe the behavior of the different obstacles along time. Previously scanned obstacles are stored and checked with the new information available.
Before high level processing, egomotion correction is performed according to the movement of the car during last detection, as explained in the previous section (eq. 2 to 5). Thus all the previously detected obstacles can be referenced to actual vehicle position.
Movement of pedestrians detected in previous scans is computed thus the following position is predicted for every obstacle. Obstacles are searched within a window according to the size of each obstacle. If several obstacles have been found only the most similar according to several parameters is considered. This comparison process is carried out according to shape characteristics, i.e. the width and position.
In subsequent scans if a pedestrian obstacle is classified whether as a small obstacle or as a pedestrian by low level it is considered a pedestrian if it satisfies some constraints relative to its movement and size. This procedure allows tracking a pedestrian even when it does not satisfies the pedestrian models shown in figure 5.
For each obstacle, a record of the latest 10 low level detection is stored to give a higher level detection. This higher level detection takes into account ten movements using eq. 8.

$$V_i = \delta_i N_i \tag{8}$$

here V_i represents the number of votes for each type of obstacle, δ_i is a gain factor associated with each obstacle, and N_i is the number of times that an obstacle has been considered as being this type during last ten low level detections. Higher level classification chooses the higher V_i for all possible classes of obstacles.

$$p = 100 \cdot \frac{V_i}{(10 \cdot \delta_i)} \tag{9}$$

According to the p formula (eq. 9), for values where the occurrence is 10, the certainly (p) will be 100%.

4.2 Far Infrared Subsystem

The proposed system makes use of raw images of the microbolometer, obtained through a 14 bit A/D. The gray level of each pixel of these images represents the amount

of heat that the sensor captures. The camera used is based on the non-refrigerated microbolometer and, as such, its sensibility changes in a way that is function of its temperature. It is necessary, then, to calibrate that sensibility.

The camera is modeled as a pin-hole. The intrinsic characteristics are known and so is the position and orientation of the camera.

The homography of the ground plane onto the sensor is calculated for each frame (eq. 13) to determine the position. The projection of a 3D point in the image plane can be done if it is known its relative position to a certain plain. Camera position related to the ground is known considered constant. The rotation of the camera is known via the gyroscopes included in MTI-G previously introduced.

$$\begin{bmatrix} U \\ V \\ S \end{bmatrix} = P \cdot W \begin{bmatrix} X \\ Y \\ Z \\ S \end{bmatrix} \tag{10}$$

where P is the intriniscs matrix. The camera movement between frames is modelled as W, which is comprised of the rotation matrix R and the translation vector T from the camera coordinate system to the ground. U and V are the image homogenous coordinates, being the true pixel coordinates u=U/S and v=V/S.

$$P = \begin{bmatrix} f_u & 0 & c_u \\ 0 & f_v & c_v \\ 0 & 0 & 1 \end{bmatrix} \tag{11}$$

$$W = [R \quad T] = \begin{bmatrix} 1 & 0 & 0 & 0 \\ 0 & cos(\frac{\pi}{2} + \theta) & -sin(\frac{\pi}{2} + \theta) & t_y \\ 0 & sin(\frac{\pi}{2} + \theta) & cos(\frac{\pi}{2} + \theta) & 0 \end{bmatrix} \tag{12}$$

The results of the projection of a world point in the image plane are especially sensitive to variations of the skew angle θ. In the presented system this angle is known for each capture frame with the help of an accelerometer with three degrees of freedom attached to the same base as the camera, these accelerometers are also included in MTI-G system form xsens. A point on the ground plane is projected on the image as:

$$u = c_u - \frac{X \cdot f_u}{Y \cdot sin(\frac{\pi}{2} + \theta)} \tag{13}$$

$$v = c_v - \frac{t_y \cdot f_v}{Y \cdot sin(\frac{\pi}{2} + \theta)} - \frac{f_v}{tan(\frac{\pi}{2} + \theta)} \tag{14}$$

where f_u and f_v are the focal lengths on the u and v directions of the image; c_u and c_v are the coordinates of the center of the images. These four parameters are measured in pixels.

The intrinsic are obtained in a calibration process that involves the use of a special chessboard pattern, a matrix of incandescent lamps.

Finally, knowing that the image coordinates are $u = \frac{U}{S}$ and $v = \frac{V}{S}$. The relation between those and the world coordinates of the ground plane can be calculated with eq. 13 and 14.

ROI check

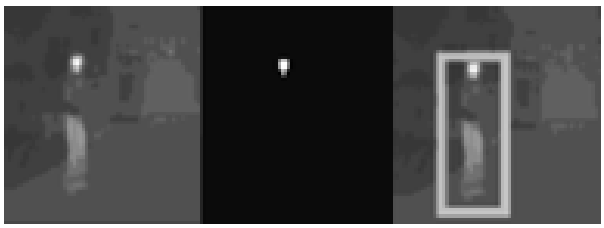

A B C

Figure 6. (A) Image received from the camera. (B) Binarized image with a head. (C) ROI selected.

Extraction of the warm areas is done by thresholding the image in two times: the first threshold tries to detect the heads of the pedestrians in the images giving regions of interest; second time, the whole pedestrian silhouette is searched.

Objects within the normal temperature of the human body are thresholded. The result is a binarized image, containing blobs that can represent parts of the human bodywith a high temperature difference, especially heads and hands (figure 6). Since this first phase searches for the human heads, only blobs in the upper half of the image are taken into account. Also blobs that are not within a reasonable size are also excluded.

ROIs found by laser scanner was taken into account in a first approach given the truthiness of laser scanner sensors. In this first approach heads where searched only in regions given by the laser. Results showed that there were errors in segment given by the laser, mainly when several pedestrians were presented at short distances. So finally a subsequent implementation was created that took into account both ROIs given by the laser and heads detected by the FIR camera thus missdetection due to a bad thresholding when looking for heads where avoided, and also missdetection due to bad laser segmentation.

Once the head candidates have been selected, a first set of regions of interest are generated and a bounding box created. Top of the box is chosen highest point of the head, while the lowest point is at the closest point of the ground at that resolution. This way, the whole body of the pedestrian is included in the box, if there is any (figure 6). The width of the bounding boxes is set to be 3/7 of the height, as it is a usual proportion of the human body. This width is big enough to accommodate inside pedestrians of all sizes. At this point only the position of the head in the image is known, thus these bounding boxes have to be big enough to contain any pedestrian, no matter what height. A first approach is to suppose that the head is 200cm from the ground plane on which the pedestrian is walking. The distance of the pedestrian to the camera is given by eq. 15, where w_z = 2m. The base of the region of interest is calculated with eq. 15, for this new distance. The width of

the bounding boxes is set to be 3/7 of the height, as it is a usual proportion of the human body.

$$w_y = \frac{(w_z - h) \cdot \alpha_u}{v - v_0} \quad (15)$$

A second set of region of interest is created using information given by the laser. If this region has no correspondence with far infrared region detected, new boxes are created. With laser information width is provided, but no height. An inverse proceeding is performed taking into account that height is 7/3 times the width.

Figure 7. Binarization inside the ROI previously founded.

The regions of interest generated from the original image are now binarized with a threshold that is the lower temperature established for the human body. Since most pedestrians' height is less than 190 cm. Bounding boxes are resized to fit the detected silhouette, assuming that the lowest part of the pedestrian are the feet, and that those are resting on the flat ground ahead the vehicle (figure 7).
Vertical Symmetry Pedestrians edges on far infrared images are usually very well defined against a cool background. Human beings present a very high vertical symmetry, so it can be used to separate them from the non-pedestrian class. Edges are extracted using a vertical Sobel filter, both for positive and negative borders. Only the ROIs obtained in previous steps of the algorithm are considered, so vertical edges of each pedestrian have to be symmetrical around an axis located approximately at $w_i/2$, where w_i is the width of each ROI_i.
Eq. 16 defines this symmetry, normalized by the size of the box.

$$S = \sum_{i=0}^{h} \left[\sum_{j=0}^{w} \left(I_P \left(i, \frac{w}{2} + j \right) \cdot \left(I_N (i, \frac{w}{2} - j \right) \right) \right] \cdot \frac{1}{w \cdot h} \quad (16)$$

where I_P and I_N are the images of the positive and negative Sobel filter, respectively; w and h are the width and height of the ROI. If the symmetry S is not over a certain threshold, the ROI is discarded.

Correlation with non-deformable models

Final verification of the extracted regions is done by means of gray scale correlation with some precomputed models. Correlation takes place between the final ROIs extracted thresholded and the models, whose creation process is explained in eq. 17.

$$S = \sum_{i=0}^{N} \frac{R_i(x,y)}{N} \quad (17)$$

where N is the number of ROIs selected for the creation of each model. In this case, every model has been generated out of N = 50 candidates.

a b c d e

Figure 8. Pedestrian models.

Pedestrian's main difference is due to the position of the legs. That is why those ROIs that eventually contain a pedestrian are grouped in four different categories: open, almost open, almost closed and closed legs. An example of these models can be seen on figure 8 (a to d). This approach enables the algorithm to correctly identify a wider diversity of shapes but it takes longer to process four correlations for each candidate. To reduce the number of calculations a fifth model is created for a common characteristic of pedestrians: the head. An example of this model can be seen on figure 8 (e). For each candidate, the top third of the bounding box is correlated with this head model before carrying on with the other four.
If there is not a satisfactory score, the region is deleted. Besides computational time improvement, the use of this head model can prevent misdetections of due occlusions, i.e. standing behind a parked car. In those cases only the upper half of the person is visible and would return a negative from a full-body model correlation.
Pedestrians located close to the camera present very rich details on the image, as far as long wave infrared vision goes. However, as this distance increases, the contour gets softer and the overall appearance of the candidates changes. To take account of all distances, four sets of the previous model have been created. Correlation will only take place between the candidate and the set of models created for that particular range of distances, in which the candidate is. Models have been created for four distance ranges: 5 to 15m, 15 to 25m, 25 to 40m.
Correlation is done by eq. (18), introduced in [17]:

$$c = \frac{\sum_{i=0}^{N} [(p(x,y)_i - 0.5)(M(x,y)_i - 0.5)]}{\sum_{i=0}^{N} [(p(x,y)_i - 0.5)]} \quad (18)$$

where p(x, y) is each pixel of candidate ROI and M (x, y) is each pixel of the model.

Tracking stage

An Unscented Kalman Filter was used to perform tracking in FIR stage. The Unscented Kalman Filter (UKF) [18] and [19] extends the general Kalman filter to non-linear

transformations of a random variable without the need of linearization, as the Extended Kalman Filter (EKF) in eq. (13) and (14), this transformation is highly non-linear. Thus, the use of the UKF is justified over the EKF, achieving better results with approximately the same computational demands.

5 Fusion Algorithm

Information received by both subsystems is based on probabilities of being a pedestrian. Using this information a fusion scheme has been developed.

Before being able to fuse the results given by both subsystems, a coordinate association is mandatory. Laser coordinate system was considered as reference due to its higher trustworthiness. So obstacles are referred to the bumper of the car where the LIDAR was mounted.

Fusion sensor calibration is performed using Least Mean Square (LMS) algorithm. The calibration algorithm detects pedestrians with both subsystems at the same time and a LMS algorithm is used to obtain the coefficients to convert coordinates from FIR coordinate system to laser scanner coordinate system.

At this point a feature vector can be obtained using information from both subsystems. These features are velocity, probability from FIR subsystem, probability from laser scanner subsystem, width (from each subsystem), position (x,y), and previous detection results. They were introduced in an AdaBoost decision tree to perform the final decision based on both high level and low level information.

Figure 9. Vehicle IVVI 2.0.

6 Results and Conclusions

A fusion method has been presented taking advantage of FIR and the laser scanner possibilities. The algorithm has been tested in the platform IVVI 2.0 (figure 9). As mentioned in the first part of the present work, this work is the first approach to data fusion for the vehicle IVVI 2.0. It performs level 0 and level 1 of JDL model data fusion. Level 2 is achieved after obstacles classification. Subsequent works will focus in the integration of other information sources. Also level 3 will be implemented by future trajectories prediction o avoid dangerous road situation. Devices used for this approach were a SICK laser LMS 291 mounted in the bumper and a FIR camera Flir Indigo Omega with sensitivity between the 7.5µm and 13.5µm.

Results obtained for every subsystem are a detection percentage of 90%. Fusion regions results show that more than 96% of pedestrian has been detected.

Acknowledgements

This work also was supported by the Spanish Government through the CICYT projects VISVIA (Grant TRA2007-67786-C02-02) and POCIMA (Grant TRA2007-67374-C02-01).

References

[1] A. Polychronopoulos, A. Amditis, "Revisiting JDL model for automotive safety applications: the PF2 functional model," Information Fusion, 2006 9th International Conference on , vol., no., pp.1-7, 10-13 July 2006.

[2] White, F.E., "A Model for Data Fusion", Proc. 1st National Symposium on Sensor Fusion, 1988.

[3] Llinas, L., Bowman, C., Rogova, G., Steinberg, A., Waltze, E., White, F., "Revisiting the JDL Data Fusion Model II", published at www.infofusion.buffalo.edu.

[4] C. Premebida, O. Ludwig and U. Nunes. “LIDAR and vision-based pedestrian detection system” in Journal of Field Robotics, vol. 26 Issue 9. Wiley, Sep. 2009. pp 696-711.

[5] N. Floudas, A. Polychronopoulos, O. Aycard, J. Burlet and M. Ahrholdt, "High Level Sensor Data Fusion Approaches For Object Recognition Road Environment," Intelligent Vehicles Symposium, 2007 IEEE , vol., no., pp.136-141, 13-15 June 2007.

[6] N. Kaempchen and K. Dietmayer, “Fusion of laserscanner and video for advanced driver assistance systems,” in Proceedings of ITS 2004, 11th World Congress on Intelligent Transportation Systems, Nagoya, Japan, October 2004.

[7] O. Aycard,A. Spalanzani, J. Burlet, C. Fulgenzi, Dung Vu; D. Raulo, M. Yguel, "Grid Based Fusion & Tracking," Intelligent Transportation Systems Conference, 2006. ITSC '06. IEEE , pp.450-455, 17-20 Sept. 2006.

[8] L. Spinello and R. Siegwart, (2008, May). “Human detection using multimodal and multidimensional features”. In IEEE International Conference on Robotics and Automation, 2008. ICRA 2008, Pasadena, CA (pp. 3264-3269).

[9] C. Premebida, O. Ludwig and U. Nunes . “Exploiting LIDAR-based Features on Pedestrian Detection in Urban Scenarios”. In: Proc. of the IEEE ITSC 2009, USA.

[10] R. Labayrade, C. Royere, D. Gruyer, and D. Aubert, D. “Cooperative Fusion for Multi-Obstacles Detection

With Use of Stereovision and Laser Scanner". Auton. Robots 19, 2 .Sep. 2005, 117-140.
[11] M. Mahlisch, R. Hering, W. Ritter and K. Dietmayer, "Heterogeneous Fusion of Video, LIDAR and ESP Data for Automotive ACC Vehicle Tracking," Multisensor Fusion and Integration for Intelligent Systems, 2006 IEEE International Conference on, pp.139-144, Sept. 2006.
[12] A. Broggi, P. Cerri, S. Ghidoni, P. Grisleri, Ho Gi Jung, "Localization and analysis of critical areas in urban scenarios," Intelligent Vehicles Symposium, 2008 IEEE , pp.1074-1079, 4-6 June 2008.
[13] N. Kaempchen, M. Buehler and K. Dietmayer, "Feature-level fusion for free-form object tracking using laserscanner and video," in Intelligent Vehicles Symposium, 2005. Proceedings. IEEE , pp. 453-458, 6-8 June 2005.
[14] F. Nashashibi and A. Bargeton, "Laser-based vehicles tracking and classification using occlusion reasoning and confidence estimation," Intelligent Vehicles Symposium, 2008 IEEE, pp. 847–852, June 2008.
[15] F.Garcia, P. Cerri, A. Broggi, J. M. Armingol and A. de la Escalera, "Vehicle Detection Based on Laser Radar". Lecture Notes in Computer Science. Computer Aided System theory. Eurocast 2009. 393-397.
[16] F. Garcia, F. Jiménez, J. E. Naranjo, J. G. Zato, F. Aparicio, J. M. Armingol and A. de la Escalera. "Analysis of LIDAR sensors for new ADAS applications. Usability in moving obstacles detection". ITS World Congress 2009. Stockholm.
[17] D. Olmeda, C. Hilario, A. de la Escalera, and J. M. Armingol. "Pedestrian detection and tracking based on far infrared visual information". Advanced Concepts for Intelligent Vision Systems, 2008.
[18] S Julier and J Uhlmann. "A new extension of the kalman Filter to nonlinear systems. Int. Symp". Aerospace/Defense Sensing, Jan 1997.
[19] M. Meuter, U. Iurgel, S. Park, and A. Kummert. "The unscented kalman filter for pedestrian tracking from a moving host". Intelligent Vehicles Symposium, Jan 2008.